Theoretical Study of the Electronic Structure of 2,2′-Bisilole in Comparison with 1,1′-Bi-1,3-cyclopentadiene: σ^*–π^* Conjugation and a Low-Lying LUMO as the Origin of the Unusual Optical Properties of 3,3′,4,4′-Tetraphenyl-2,2′-bisilole[1)]

Shigehiro Yamaguchi and Kohei Tamao*

Institute for Chemical Research, Kyoto University, Uji, Kyoto 611

(Received March 14, 1996)

The purpose of this work is the theoretical elucidation of the origin of the unusually long UV-vis absorption maximum, λ_{max} = 398 nm, of 3,3′,4,4′-tetraphenyl-2,2′-bisilole, which we have observed recently. Several semiempirical and ab initio calculations have been performed for some model compounds, silole and 2,2′-bisilole, in comparison with their carbon analogs, cyclopentadiene and 1,1′-bi-1,3-cyclopentadiene, respectively. The PM3 calculations indicate that the silole ring has a considerably low-lying LUMO, arising from σ^*–π^* conjugation between a π-symmetry σ^* orbital of the exocyclic σ bonds on silicon and a π^* orbital of the butadiene skeleton. Ab initio calculations at the CIS/6-31G* level of theory suggest that the experimental large differences in the absorption maximum in the UV-vis spectra between the bisilole and the bicyclopentadiene derivatives are ascribed also to the low-lying LUMO level of the bisilole compared with the bicyclopentadiene. It is further demonstrated that the σ^*–π^* conjugation is enhanced by the molecular distortions, twisting and folding, of the bisilole skeleton present in the X-ray structure, resulting in the lowering of the LUMO level. The calculated data are supported by the redox potentials of some representative compounds, as determined by cyclic voltammetry measurements. The σ^*–π^* conjugation and the low-lying LUMO would thus be the origin of the unusual optical properties of bisilole derivatives.

Polysiloles **1**, silole (sila-2,4-cyclopentadiene) 2,5-linked π-conjugated polymers, are still veiled, but promising targets for development of novel π-electronic organic materials.[2—6)] Some theoretical calculations on the polysiloles have suggested their low bandgaps (ca. 1.4 eV),[3)] nonlinear optical properties,[4)] and thermochromism.[5)] Recently we have succeeded in preparing oligosiloles, from dimer **2** to tetramer **3**, as model compounds of polysiloles (Chart 1).[7)] Of special note, 3,3′,4,4′-tetraphenyl-2,2′-bisilole **2a**, a silole dimer, has a considerably long absorption maximum (λ_{max} 398 nm) in the UV-vis spectra among some conjugated dimers of five-membered cyclic dienes.[8)] In order to compare the properties of the bisilole with its carbon analog, we have quite recently also prepared 1,1′-bi-1,3-cyclopentadiene (hereafter, abbreviated to bicyclopentadiene) derivatives **4** having almost the same substituents as **2**.[9)] The difference in λ_{max} between **2a** and **4a** (λ_{max} 340 nm) has been found to reach 58 nm. We have thus carried out theoretical calculations to elucidate the electronic structure of bisilole in detail in comparison with that of bicyclopentadiene. This report describes the calculation results on the parent silole and bisilole as well as cyclopentadiene and bicyclopentadiene.

Results and Discussion

Structural Comparison between Bisilole 2a and Bicyclopentadiene 4b. Crystal structures of bisilole **2a**[7)] and 4,4′-diiodobicyclopentadiene **4b**[9)] and their structural parameters have been reported previously. The stereoviews of the two five-membered rings are shown for both compounds in Fig. 1, because the structural aspects of these skeletons are important for the present discussion. In the crystal structures of **4b**, a 1 : 1 mixture of *anti* and *syn* forms is observed.

There are two kinds of distortion, as illustrated in Fig. 2. One is the *twisting* about the connecting C2–C2′ bond, defined by the torsion angle θ. The other is the *folding* of two rings from the C2–C2′ bond in the same direction, defined by the folding angle ω between the mean plane of a ring and the connecting bond. The characteristic features are as follows: Bisilole **2a** is highly twisted with torsion angle $\theta = 62°$ and is folded with an averaged folding angle $\omega = 15°$. Both conformers of bicyclopentadiene **4b** are also highly twisted, but have smaller folding angles than **2a**; the *anti* form has $\theta = 70°$ and $\omega = 2°$ and the *syn* form $\theta = 118°$ and $\omega = 10°$.

UV-vis Spectral Data for Bisilole 2a and Bicyclopentadiene 4a. UV-vis absorption data for bisilole **2a** and bicyclopentadiene **4a** are summarized in Table 1, which also contains the data for the parent silole **5**[10)] and cyclopentadiene **6** (Chart 2).[11)] Two comparisons will be made.

(1) Silicon vs. carbon: Silole **5**, recently isolated and characterized by Michl and his co-workers, has a longer absorption maximum by 21 nm than carbon analog **6**.[10)] Similarly, the λ_{max} of bisilole **2a** is 58 nm longer than that of bicyclopentadiene **4a**.[9)] This difference corresponds to 0.53 eV.

(2) Mono-ring vs. two-ring: There is a considerably large

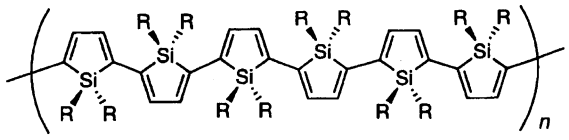

1

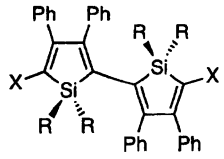

2a (R = *i*-Pr, X = H)
2b (R = Et, X = Br)

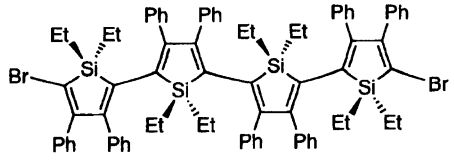

3

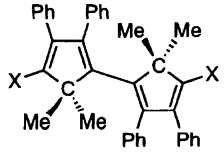

4a (X = H)
4b (X = I)

Chart 1.

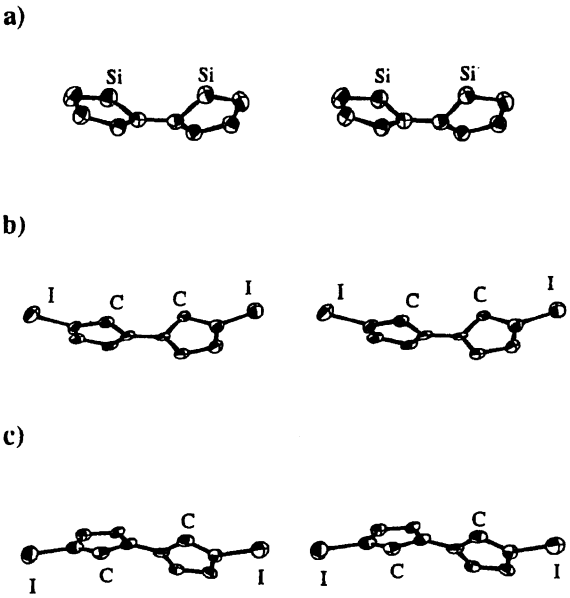

Fig. 1. Crystal Structures of bisilole **2a** and diiodobicyclopentadiene **4b**: Stereoviews of **2a** (a), *anti* conformer of **4b** (b), and *syn* conformer of **4b** (c). Phenyl groups and alkyl groups are omitted for clarity. All of the drawings are 50% thermal probability.

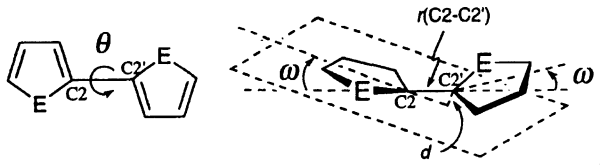

(E = SiH_2 or CH_2)

Fig. 2. Definitions of the torsion angle θ, from *anti* arrangement of the two rings, and the folding angle ω (average value), that is an angle between the mean plane of a five-membered ring and the connecting bond C2–C2′, as defined by $\sin\omega = d/r(\text{C2–C2}')$, where d stands for the displacement of one connecting carbon atom from the mean plane of the other ring and r(C2–C2′) is the bond length of the connecting bond.

Table 1. UV-vis Absorption Data of Silole and Cyclopentadiene Derivatives

Compound		λ_{max}/nm	log ε
Silole[a)]	**5**	278	—
Cyclopentadiene[b)]	**6**	257	—
Bisilole[c,d)]	**2a**	242[e)]	4.51
		398	3.71
Bicyclopentadiene[c,f)]	**4a**	249[e)]	4.53
		340	3.43

a) Ref. 10. b) Ref. 11. c) In chloroform. d) Ref. 7. e) Absorptions around 240 nm can be assigned to π–π^* transitions of phenyl groups. f) Ref. 9.

5 **6**

Chart 2.

bathochromic shift, more than 120 nm, upon changing from monosilole **5** to bisilole **2a**, while in the carbon analogs there is a bathochromic shift of only about 80 nm from **6** to **4a**. All the data strongly suggest development of a unique π-electronic structure by the combination of two silole rings.

In addition, it has previously been observed that bisiloles **2a** and **2b** and bicyclopentadienes **4a** and **4b** have twisted structures not only in the solid state but also in solution, as confirmed by NMR studies, and, in consonant with this, bisilole **2b** has almost the same absorption maximum both in the solid state (λ_{max} 416 nm) and in solution (λ_{max} 417 nm).[7)]

Theoretical Study of the Electronic Structure of Bisilole in Comparison with Bicyclopentadiene. (a) Comparison of the Electronic Structures between Silole and Cyclopentadiene. Some research groups have already reported theoretical analyses for the electronic structure of the parent silole **5**.[10,12)] Michl et al. have recently characterized the spectral data for **5** in detail by ab initio calculations and pointed out that the longer λ_{max} of silole in comparison with cyclopentadiene is probably due to an increased cyclic hyperconjugation in **5**.[10)] To clarify the role of the silicon atom

in the electronic structure of the silole ring, we have now compared the electronic structure of silole with that of cyclopentadiene based on HF/6-31G* calculations, the results being shown in Fig. 3. The silole has a lower-lying HOMO (highest occupied molecular orbital) by about 0.4 eV and a much lower-lying LUMO (lowest unoccupied molecular orbital) by about 1.3 eV than cyclopentadiene has. More significantly, silole has a lobe on silicon in-phase with lobes on the adjacent ring carbons in the LUMO, while cyclopentadiene has no such a lobe on carbon but a butadiene-like LUMO only. This aspect has already been reported,[5,12c,12e] but the origin of the "*in-phase lobe on silicon*" has not been clarified.

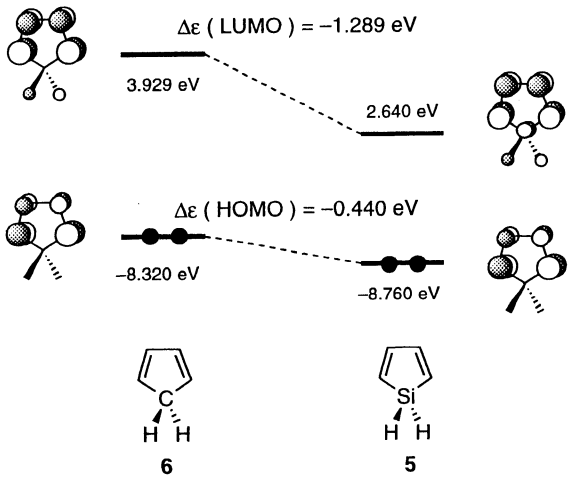

Fig. 3. Relative energy levels of the HOMO and LUMO for silole **5** and cyclopentadiene **6**, based on the HF/6-31G* calculations.

The origin has now been clearly disclosed by an orbital correlation diagram based on semiempirical PM3 calculations on 1,1-dimethylsilole **7**, as shown in Fig. 4.[13] Thus, silole **7** is tentatively divided into a butadiene moiety (1,3-butadiene) and a dimethylsilylene moiety (dimethysilane). The correlation between four π orbitals of the butadiene moiety and two σ orbitals of the dimethylsilylene moiety brings about six π orbitals for silole. Most importantly, the low-lying LUMO in silole arises from mixture of the σ^* ($2b_1$) orbital of the dimethylsilylene moiety with the π^* ($3b_1$) orbital of the butadiene moiety, that is, σ^*–π^* *conjugation*.[14,15] Thus, *the origin of the "in-phase lobe on silicon" turns out to be the π-symmetry σ* orbital of the exocyclic two Si–C σ bonds*. The σ^*–π^* conjugation may arise from the fixed perpendicular arrangement of the plane of the dimethylsilylene moiety to the plane of the butadiene moiety and the energetically comparable σ^* and π^* orbitals. Indeed, in the case of the carbon analog, 5,5-dimethyl-1,3-cyclopentadiene, the σ^*–π^* conjugation in the LUMO is almost negligible be-

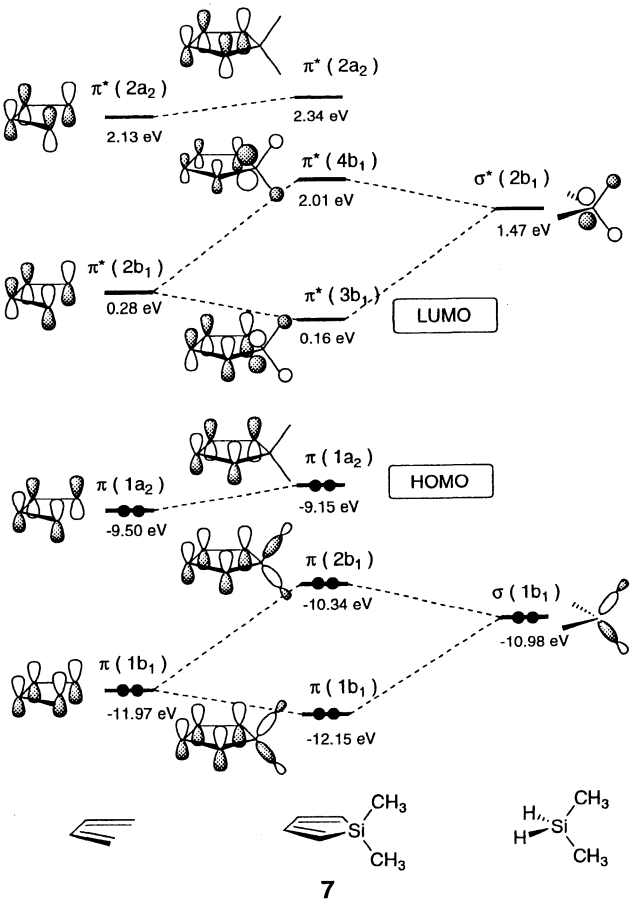

Fig. 4. Orbital correlation diagram for 1,1-dimethylsilole **7**, based on the PM3 calculations.

cause of the higher energy level of the corresponding exocyclic C–C σ* orbital.[16] The shape of the LUMO of silole is visualized in Fig. 5, together with that of cyclopentadiene for comparison.

(b) Comparison of the Relative HOMO and LUMO Energy Levels between Bisilole and Bicyclopentadiene. To elucidate the large difference in λ_{max} between bisilole **2a** and bicyclopentadiene **4a**, we have carried out ab initio calculations on the model compounds, i.e., parent bisilole **8** and its carbon analog **9** using the CIS procedure implemented in the Gaussian 92 program with the 6-31G* basis set. The results are summarized in Table 2. In view of the twisted structures of **2** and **4** both in solution and in the solid state, we first performed calculations for **8** and **9** employing geometries derived from the X-ray crystal structures of **2a** and **4b** (*anti* and *syn* conformers), respectively. The calculated $\Delta\lambda_{max}$(**8**−**9**) reaches 49—60 nm, which corresponds to $\Delta\Delta E$(**8**−**9**)=0.90—1.15 eV (compare Entries 1 with 8 or 9), where ΔE denotes an excitation energy. The relative HOMO and LUMO energy levels for **8** and **9** (*anti* conformer) are shown in Fig. 6. Bisilole **8** has a slightly lower-lying HOMO by about 0.06 eV and a much lower-lying LUMO by about 1.5 eV than the *anti* conformer of the bicyclopentadiene **9**. We could thus deduce that the longer λ_{max} of **2a** than that of **4a** is mainly due to the considerably lower level of the LUMO of the bisilole.

When the coplanar conformations were employed for **8** and **9**, only 0.39 eV of the $\Delta\Delta E$ (**8**−**9**) was observed (Entries 2 and 10). These results imply that the distortions present in the crystal structure of bisilole **2a** may be responsible for the

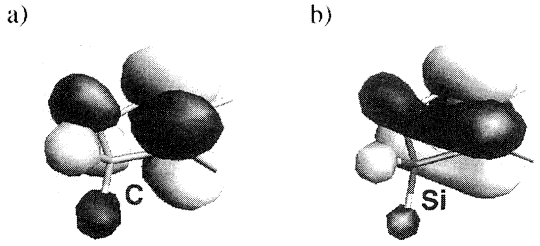

Fig. 5. MO drawings of the LUMO for (a) cyclopentadiene **6** and (b) silole **5**, the threshold level being 0.050.

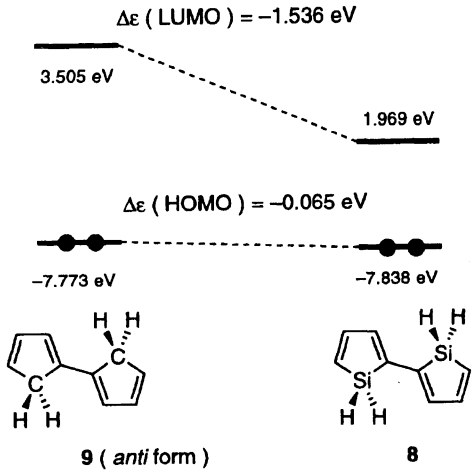

Fig. 6. Relative energy levels of the HOMO and LUMO for bisilole **8** and bicyclopentadiene **9**, calculated employing the geometries derived from the X-ray structures.

Table 2. CIS Calculations on Bisilole and Bicyclopentadiene[a]

Entry	Compound	θ and ω[b]	λ_{max} (calcd)	ΔE[c]	ε (HOMO)[d]	ε (LUMO)[d]	$\Delta\varepsilon$[e]
		deg	nm	eV	eV	eV	eV
1		X-ray	287	4.320	−7.838	1.969	9.797
2	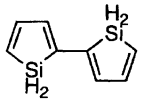	θ=0, ω=0	294	4.216	−7.591	1.825	9.416
3		θ=0, ω=15	299	4.150	−7.542	1.825	9.367
4		θ=60, ω=0	270	4.589	−7.967	2.170	10.137
5	**8**	θ=60, ω=5	269	4.606	−7.956	2.209	10.165
6		θ=60, ω=10	269	4.606	−7.935	2.243	10.178
7		θ=60, ω=15	280	4.434	−7.935	2.020	9.955
8		X-ray (*anti*)	227	5.466	−7.773	3.505	11.278
9	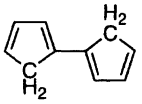	X-ray (*syn*)	238	5.216	−7.571	3.381	10.952
10		θ=0, ω=0	269	4.610	−7.086	2.743	9.829
11		θ=70, ω=0	226	5.482	−7.731	3.515	11.246
12	**9**	θ=120, ω=0	242	5.125	−7.426	3.209	10.635
13		θ=120, ω=10	235	5.278	−7.618	3.306	10.924
14		θ=60, ω=0	234	5.298	−7.560	3.351	10.911
15		θ=60, ω=5	234	5.290	−7.535	3.364	10.899
16		θ=60, ω=10	236	5.262	−7.501	3.368	10.869
17		θ=60, ω=15	238	5.215	−7.459	3.363	10.822

a) In entries 1, 8, and 9, one point CIS/6-31G* calculations were conducted with employing the geometries derived from X-ray crystal structure data of **2a** and **4b** for **8** and **9**, respectively, hydrogen atoms being fully optimized at the HF/6-31G* level of theory. In Entries 2 and 10, calculations were performed at the CIS/6-31G*//HF/6-31G* level of theory, in which geometries were optimized under C_{2h} symmetry constraints. In other cases, one point CIS/6-31G* calculations were conducted using the optimized geometries in Entries 2 or 10 with changing only the θ and ω values. b) Defined in Fig. 2. c) Excitation energy. d) Energy levels of HOMO or LUMO. e) HOMO–LUMO energy gap: ε(LUMO) − ε(HOMO).

large difference in λ_{max} between **2a** and **4a**.

(c) Effect of Twisting and Folding on the LUMO Level of Bisilole. Several calculations on **8** and **9** were further performed at the CIS/6-31G* level of theory in order to elucidate the effect of the distortions, twisting and folding, on the LUMO of bisilole. The two angles, θ and ω, were changed in light of the experimental data. The results listed in Table 2 are summarized as follows.

(1) As mentioned above, calculations on coplanar conformers, $\theta = \omega = 0°$, afford a small $\Delta\Delta E$ (**8** − **9**) = 0.39 eV (Entries 2 and 10). When the folding $\omega = 15°$ is further applied to the coplanar conformation for **8**, little change in λ_{max} is observed (Entry 3). (2) Only the twisting is applied, i.e., $\theta = 60°$ for **8** and 70° or 120° for **9** keeping $\omega = 0°$ for both, resulting in a larger $\Delta\Delta E$ (**8** − **9**) = 0.54—0.89 eV (Entries 4, 11, and 12). (3) Folding angles similar to those observed experimentally are further applied to these twisted conformers, i.e., $\theta = 60°$, $\omega = 15°$ for **8** (Entry 7) and $\theta = 70°$, $\omega = 0°$ or $\theta = 120°$, $\omega = 10°$ for **9** (Entries 11 and 13), affording $\Delta\Delta E$ (**8** − **9**) = 0.84—1.05 eV. These theoretical results are visualized in Figs. 7 and 8, which show the angle-dependent variations of the HOMO and LUMO levels in the bisilole and the bicyclopentadiene and the deformation of the shape of the LUMO, respectively. The exceptional behavior of the LUMO level of bisilole is noted.

All these results are reasonably explained as follows. First, for the coplanar conformation (Fig. 7a), the σ*–π* conjugation in the LUMO of bisilole becomes less efficient in comparison with that in monosilole, because, in the coplanar bisilole, a larger energy gap between the σ* and the π* levels results from considerable lowering of the π* level owing to the extended π-conjugation in the bis-butadiene moiety. π-Conjugation in bisilole and bicyclopentadiene may thus be comparable, resulting in only a small $\Delta\Delta E$ (**8** − **9**). The less efficient σ*–π* conjugation in the coplanar bisilole is represented as the slimmed lobes on silicon in Fig. 8b. Second, when twisting is applied, the $\Delta\Delta E$ (**8** − **9**) becomes larger, because the level-up of the LUMO in bisilole is smaller than in bicyclopentadiene (Fig. 7b). The smaller level-up is probably due to the greater contribution of the σ*–π* conjugation in the LUMO of the twisted bisilole than that in the coplanar one. In other words, the twisting makes the π-conjugation over the bis-butadiene moiety much less efficient to bring the π* orbital level up closer to the σ* orbital level, resulting in larger interaction between both orbitals, i.e., more efficient σ*–π* conjugation. This is visualized in Fig. 8c as the re-

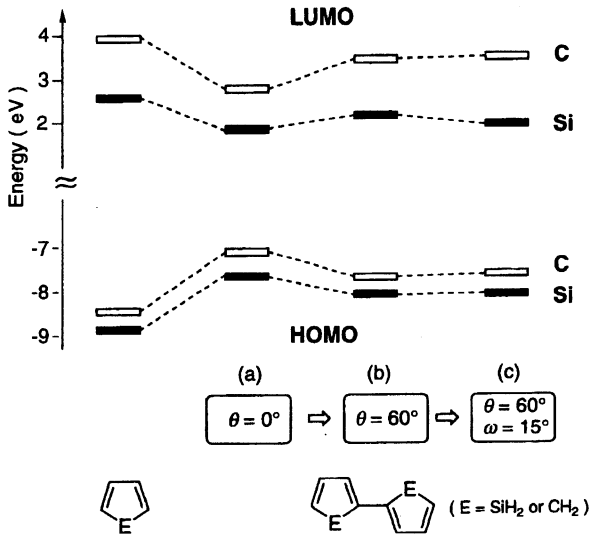

Fig. 7. Change of the HOMO and LUMO energy levels of bisilole (□) and bicyclopentadiene (■) by twisting and folding. Energy levels of the corresponding monomers are also shown for comparison.

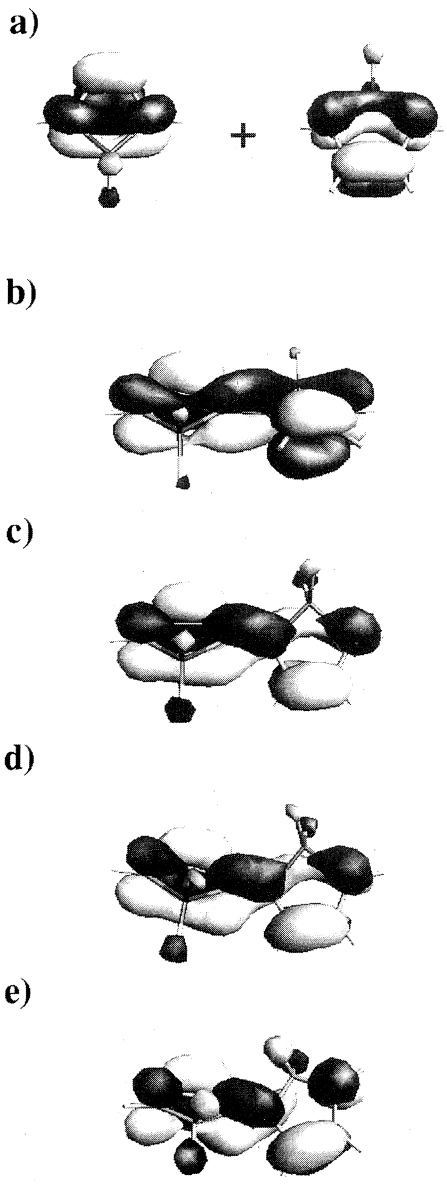

Fig. 8. Deformation of the LUMO of bisilole **8** and bicyclopentadiene **9**, accompanied by the change of the θ and ω values; a) two silole rings, b) $\theta = \omega = 0°$ for **8**, c) $\theta = 60°$, $\omega = 0°$ for **8**, d) $\theta = 60°$, $\omega = 15°$ for **8**, and e) $\theta = 60°$, $\omega = 15°$ for **9**. The threshold levels are 0.055 for silole and 0.035 for **8** and **9**, respectively.

gained lobes both on the silicon and the hydrogen atoms of the SiH_2 moiety. Third, when folding is further applied to the twisted bisilole, the $\Delta\Delta E$ (**8** − **9**) becomes larger to be close to that obtained by employing the geometries derived from the crystal structures, mainly due to the lowering of the LUMO level of the bisilole (Fig. 7c). It should be noted that when only folding is applied to the coplanar bisilole, essentially no change is observed in its HOMO and LUMO energy levels. Thus, both twisting and folding are responsible for the unique electronic structure of the bisilole.

Therefore, the effect of the folding angles in the twisted conformer was next examined. Thus, fixing the torsion angle $\theta = 60°$, only the folding angle ω was varied from 0° to 15° at 5° intervals (Table 2, Entries 4—7 for **8** and 14—17 for **9**). The energy changes in the HOMO and LUMO levels accompanied by the folding are visualized in Fig. 9. In bicyclopentadiene **9**, the folding from 0° to 15° induces a very slight but steady elevation of the HOMO level about 0.1 eV and almost no change in the LUMO level; in total, the HOMO–LUMO energy gap $\Delta\varepsilon$(**9**) is reduced by 0.09 eV. In bisilole **8**, folding up to 10° merely causes a slight elevation of the LUMO level and almost no change in the HOMO level. However, *15° folding suddenly causes the lowering of the LUMO level by 0.22 eV, while the HOMO level remains unchanged.* As a whole, folding with $\omega = 15°$ reduced the HOMO–LUMO energy gap $\Delta\varepsilon$(**8**) by 0.18 eV.[17]

The decrease in the LUMO level of the twisted bisilole by folding may be ascribed to *an enhanced* σ^*–π^* *conjugation*, as schematically represented in Fig. 10. The folding corresponds to the pyramidarization of the planar connecting carbon atom C2 (and C2′), which causes rehybridization from sp^2- to sp^3-like orbital and thus deformation of the π-orbital from pure p into sp^3-like, resulting in enlargement of a lobe of the π^* orbital in the convex side. This orbital deformation should occur also in the bicyclopentadiene; this is seen from the shape depicted in Fig. 8e. However, in the bisilole, there is the σ^* orbital on the adjacent silicon which can interact with the enlarged lobe of the π^* orbital on carbon to enhance the σ^*–π^* conjugation on the convex side. As the folding angle is increased, this σ^*–π^* conjugation is enhanced more intensively to lower the LUMO level; this is characteristic of the bisilole. The enhanced σ^*–π^* conjugation is schematically pointed out by arrows in Fig. 10, and the shape of the resulting LUMO of the distorted bisilole is visualized in Fig. 8d, which should be compared with that of the bicyclopentadiene (Fig. 8e). It is clearly indicated that there is a through-conjugation involving silicons in the convex side of the twisted and folded bisilole and this through-conjugation is characteristic to the bisilole. This may be the origin of the low-lying LUMO of the bisilole.

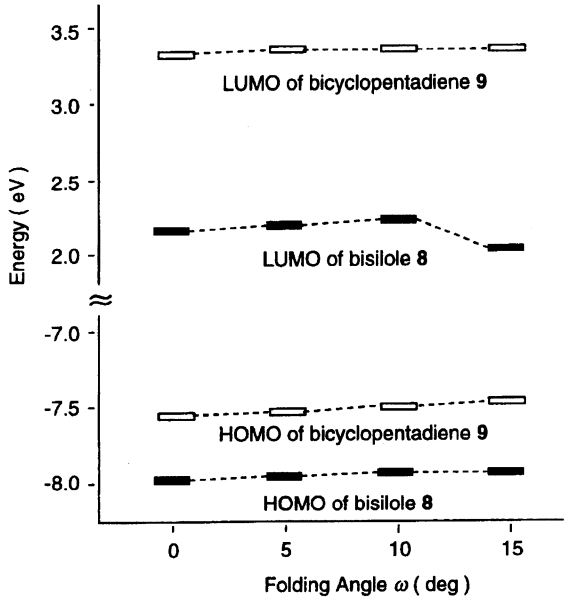

Fig. 9. Energy change of the HOMO and LUMO levels by applying folding to the twisted ($\theta = 60°$) bisilole **8** and bicyclopentadiene **9** skeleton.

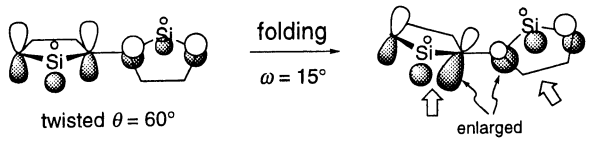

Fig. 10. Schematic drawings for the change of the LUMO of bisilole with folding of skeleton.

Redox Potentials of Bisilole and Bicyclopentadiene. The electrochemical data of some silole derivatives and their carbon analogs have been determined for comparison with the calculation results. The experimental data are summarized in Table 3. In the one-ring systems, the reduction potential (E_{pc}) of the 2,5-disilylsilole **10**[7] is about 0.5 V lower than that of carbon analog **11**,[9] while the oxidation potential (E_{pa}) of **10** is about 0.1 V higher than that of **11** (Chart 3). In the case of two-ring systems, bisilole **2a** has the

Table 3. Electrochemical Data for Silole and Cyclopentadiene Derivatives[a]

Compound		E_{pa1}, E_{pa2}/V	E_{pc1}, E_{pc2}/V
Disilylsilole	**10**	1.32	−2.45
Disilylcyclopentadiene	**11**	1.22	−2.99
Bisilole	**2a**	0.90	−2.31, −2.49
Bicyclopentadiene	**4a**	0.88, 1.06	−2.73

a) Cyclic voltammetry measurements were performed under the following condition: sample, 1 mM; solvent system, Bu_4NClO_4 (0.1 M) in acetonitrile; Ag/Ag^+ reference electrode and glassy carbon working electrode; scan rate; 100 $mV\,s^{-1}$. All redox processes were irreversible.

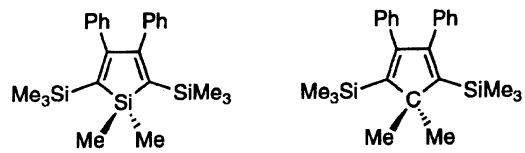

Chart 3.

first reduction potential (E_{pc1}) at about a 0.4 V lower position than that of bicyclopentadiene **4a**, whereas the first oxidation potentials (E_{pa1}) are comparable in both compounds. These data are consistent with the calculation data that silole derivatives have much lower LUMO levels and comparable HOMO levels in comparison with the carbon analogs.[18]

Conclusion

Theoretical studies have revealed that the silole ring has an unusually low-lying LUMO level arising from σ^*–π^* conjugation. This feature is recognized also in the extended π-conjugated system, bisilole. Worthy of note is that the σ^*–π^* conjugation is enhanced by molecular distortions of the bisilole skeleton, to cause a decrease in the LUMO energy level. This could be the origin of the unusual optical properties of the tetraphenyl-bisilole.

The σ^*–π^* conjugation gives siloles and their derivatives unique π-electron systems, especially in contrast to the π-electron excessive heteroaromatics such as furan, thiophene, and pyrrole. Their polymer, polysilole, would thus have quite different electronic structures and properties from those of the conventional polythiophenes, polypyrroles, and so on. Of particular interest is that the polysilole can be regarded as an *all-trans-s-cis*-polyacetylene extended with the additional σ^*–π^* conjugation. The development of these fascinating polysiloles as well as other silole-containing π-conjugated polymers[19] is now in progress in our laboratory.

Experimental

Calculations. Ground-state ab initio calculations on compounds **5**, **6**, **8**, and **9** were performed by use of the Hartree–Fock (HF) approximation with the Gaussian 92 program.[20] Geometries of **5** and **6** were optimized using the 6-31G* basis set within the constraints of C_{2v} symmetry. The excitation energies for **8** and **9** were calculated by the CIS (Configuration Interaction with Singlet Excitations) procedure[21] implemented in the Gaussian 92 program using the 6-31G* basis set. Three types of geometries were used for **8** and **9**; one optimized at the HF/6-31G* level within the C_{2h} symmetry constraints (Entries 2 and 10 in Table 2), one based on the optimized geometries changing only the θ and ω values (Entries 3—6 and 11—17 in Table 2), and one derived from the X-ray crystal structural data of **2a** and **4b** for **8** and **9**, respectively, hydrogen atoms being fully optimized at the HF/6-31G* level of theory (Entries 1, 8, and 9 in Table 2).

Semiempirical PM3 calculations using the MOPAC ver 6.0 program[22] were performed on 1,1-dimethylsilole **7**, 1,3-butadiene, and dimethylsilane Me_2SiH_2 as a silole, a butadiene moiety, and a silylene moiety, respectively, to depict an orbital correlation diagram for silole. The choice of methyl groups as the substituents on the ring-silicon atom enabled us to extract the pertinent σ-character orbital for the silylene moiety, which was impossible in the case of the parent silole as silole because of the high symmetry of silane SiH_4 as the corresponding silylene moiety.

Cyclic Voltammetry Measurements. Cyclic voltammograms were obtained by the use of a BSA CV-50W and a three-electrode cell composed of a glassy-carbon working electrode, a platinum wire counter electrode, and a Ag/0.01 M $AgNO_3$ (acetonitrile) (M = mol dm^{-3}) reference electrode. The observed potential was corrected with reference to ferrocene ($E_{1/2}$ +0.083 V) added as an internal standard after each measurement.

We thank Prof. K. Komatsu and Dr. M. Hada, Kyoto University, for CV measurements and valuable discussions. We are grateful for the financial support by Grants-in-Aid Nos. 07215240 and 07555280 from the Ministry of Education, Science and Culture, by Nagase Science and Technology Foundation, and by Ciba-Geigy Foundation (Japan) for the Promotion of Science. Computation time was provided by the Supercomputer Laboratory, Institute for Chemical Research, Kyoto University.

References

1) Silole-containing π-conjugated polymers, Part 5. For Part 4, see Ref. 9.

2) a) J. Shinar, S. Ijadi-Maghsoodi, Q. -X. Ni, Y. Pang, and T. J. Barton, *Synth. Met.*, **28**, C593 (1989); b) T. J. Barton, S. Ijadi-Maghsoodi, and Y. Pang, *Macromolecules*, **24**, 1257 (1991).

3) a) G. Frapper and M. Kertész, *Organometallics*, **11**, 3178 (1992); b) G. Frapper and M. Kertész, *Synth. Met.*, **55—57**, 4255 (1993); c) J. Kürti, P. R. Surján, M. Kertész, and G. Frapper, *Synth. Met.*, **55—57**, 4338 (1993).

4) S. Grigoras, G. C. Lie, T. J. Barton, S. Ijadi-Maghsoodi, Y. Pang, J. Shinar, Z. V. Vardeny, K. S. Wong, and S. G. Han, *Synth. Met.*, **49—50**, 293 (1992).

5) a) Y. Yamaguchi and J. Shioya, *Mol. Eng.*, **2**, 339 (1993); b) Y. Yamaguchi, *Mol. Eng.*, **2**, 311 (1994).

6) a) S. Y. Hong and D. S. Marynick, *Macromolecules*, **28**, 4991 (1995); b) S. Y. Hong, S. J. Kwon, and S. C. Kim, *J. Chem. Phys.*, **103**, 1871 (1995).

7) K. Tamao, S. Yamaguchi, and M. Shiro, *J. Am. Chem. Soc.*, **116**, 11715 (1994).

8) For comparison, several UV absorption data for non-substituted conjugated dimers of five-membered cyclic dienes are listed as follows; compound, λ_{max} (nm): 2,2′-bipyrrole, 276;[a] 2,2′-bifuran, 278;[b] 2,2′-bithiophene, 302;[b] 2,2′-biselenophene, 321;[b] 1,1′-bi-1,3-cyclopentadiene (isomeric mixtures), 352(sh), 340.[c] a) G. Zotti, S. Martina, G. Wegner, and A. -D. Schülter, *Adv. Mater.*, **4**, 798 (1992); b) R. Shabana, A. Galal, H. B. Mark, Jr., H. Zimmer, S. Gronowitz, and A. -B. Hörnfeldt, *Phosphorus, Sulfur, and Silicon*, **48**, 239 (1990); c) A. Escher, W. Rutsch, and M. Zeuenschwander, *Helv. Chim. Acta*, **69**, 1644 (1986).

9) S. Yamaguchi and K. Tamao, *Tetrahedron Lett.*, **37**, 2983 (1996).

10) V. N. Khabashesku, V. Balaji, S. E. Boganov, O. M. Nefedov, and J. Michl, *J. Am. Chem. Soc.*, **116**, 320 (1994).

11) J. Del Bene and H. H. Jaffe, *J. Chem. Phys.*, **48**, 4050 (1968).

12) a) V. Niessen, W. P. Kraemer, and L. S. Cederbaum, *Chem. Phys.*, **11**, 385 (1975); b) M. S. Gordon, P. Boudjouk, and F. Anwari, *J. Am. Chem. Soc.*, **105**, 4972 (1983); c) C. Guimon, G. Pfister-Guillouzo, J. Dubac, A. Laporterie, G. Manuel, and H. Iloughmane, *Organometallics*, **4**, 636 (1985); d) B. Goldfuss and P. V. R. Schleyer, *Organometallics*, **14**, 1553 (1995); e) K. Tamao, S. Yamaguchi, Y. Ito, Y. Matsuzaki, T. Yamabe, M. Fukushima, and S. Mori, *Macromolecules*, **28**, 8668 (1995).

13) The PM3 level calculations have also shown that the LUMO level of silole **5** is lower by 0.15 eV than that of cyclopentadiene **6**, while the HOMO levels are comparable to each other.

14) Similar σ^*–π^* conjugation has quite recently been reported to be seen in 2,2′,5,5′-tetrasila-1,1′-bicyclopentylidene: M.

Ichinohe, A. Sekiguchi, H. Sakurai, "69th Annual Meetings of the Chemical Society of Japan," Kyoto, March 1995, Abstr., 3C808.

15) A. R. Bassindale and P. G. Taylor, in "The Chemistry of Organic Silicon Compounds," ed by S. Patai and Z. Rappoport, Wiley, New York (1991), pp. 893—963.

16) Similarly, if 5,5-dimethyl-1,3-cyclopentadiene is divided into the butadiene moiety and dimethylcarbene moiety (propane), the corresponding σ^* orbital (4.04 eV) of propane lies at 2.57 eV higher level than that of dimethylsilylene moiety.

17) The final result (Table 2, Entry 7), however, does not completely reproduce the calculation results based on the X-ray structure (Table 2, Entry 1); the latter has a lower LUMO by 0.05 eV and a higher HOMO by 0.1 eV than the distorted model system. These differences are probably due to the total strain of other parts of the rings.

18) The reduction potential difference between **10** and **11** is slightly larger than that between **2a** and **4a**. This is inconsistent with the calculation results, probably due to the different substituent patterns between these two series.

19) As only one example for silole-containing (on 2,5-positions) fully π-conjugated polymers so far, thiophene–silole copolymers have been prepared by us: K. Tamao, S. Yamaguchi, M. Shiozaki, Y. Nakagawa, and Y. Ito, *J. Am. Chem. Soc.*, **114**, 5867 (1992), and Ref. 12e.

20) M. J. Frisch, G. W. Trucks, M. Head-Gordon, P. M. W. Gill, M. W. Wong, J. B. Foresman, B. G. Johnson, H. B. Schlegel, M. A. Robb, E. S. Replogle, R. Gomperts, J. L. Andres, K. Raghavachari, J. S. Binkley, C. Gonzalez, R. L. Martin, D. J. Fox, D. J. Defrees, J. Baker, J. J. P. Stewart, and J. A. Pople, "Gaussian 92," Revision A, Gaussian, Inc., Pittsburgh, PA (1992).

21) J. B. Foresman, M. Head-Gordon, J. A. Pople, and J. Frisch, *J. Phys. Chem.*, **96**, 135 (1992).

22) J. J. P. Stewart, *J. Comput. -Aided Mol. Des.*, **4**, 1 (1990).